Operational Limitations of Arctic Waste Stabilization Ponds: Insights from Modeling Oxygen Dynamics and Carbon Removal

Ragush, Colin M.; Gentleman, Wendy C.; Hansen, Lisbeth Truelstrup; Jamieson, Rob C.

Published in:
Journal of Environmental Engineering

Link to article, DOI:
10.1061/(ASCE)EE.1943-7870.0001371

Publication date:
2018

Document Version
Peer reviewed version

Operational Limitations of Arctic Waste Stabilization Ponds - Insights from Modelling Oxygen Dynamics and Carbon Removal

Colin M. Ragush, Postdoctoral Fellow
Centre for Water Resources Studies, Dalhousie University, 1360 Barrington Street, Halifax, NS, Canada, B3H 4R2
Tel.: 1-902-229-9736; Fax: 1-902-494-3108; Email: Colin.Ragush@Dal.Ca

Wendy C. Gentleman, Associate Professor
Department of Engineering Mathematics and Internetworking, Dalhousie University, 269 Morris Street PO Box 15000, Halifax, Nova Scotia, Canada, B3H 4R2
Email: Wendy.Gentleman@Dal.Ca

Lisbeth Truelstrup-Hansen, Professor
Department of Process Engineering and Applied Science, Dalhousie University, 1360 Barrington Street, Halifax, NS, Canada, B3H 4R2 Current address: National Food Institute, Technical University of Denmark, 2800 Kgs. Lyngby, Denmark
Email: ltruelst@Dal.Ca and litr@food.dtu.dk

Rob C. Jamieson, Professor
Civil and Resources Engineering Dept., Dalhousie University, 1360 Barrington Street, Halifax, Nova Scotia, Canada, B3H 4R2
Email: Jamiesrc@Dal.Ca

Abstract

Presented here is a mechanistic model of the biological dynamics of the photic zone of a single-cell arctic Waste Stabilization Pond (WSP) for the prediction of oxygen concentration and the removal of oxygen demanding substances. The model is an exploratory model to assess the limiting environmental factors affecting treatment performance in arctic WSPs. A sensitivity analysis was utilized to provide a quantification of the relative uncertainties of parameters that exist within the described modelling framework. The model was able to qualitatively reproduce mesocosm experiment trends in phytoplankton growth, dissolved oxygen concentration, and the reduction of $CBOD_5$ (Carbonaceous Biochemical Oxygen Demand – Day 5). These results demonstrated that $CBOD_5$ reduction and oxygen state are very sensitive to organic loading regimes at cool temperatures (5-15 ˚C). The sensitivity analysis identified that it was the difference in phytoplankton growth rates, and the associated change in

photosynthetic oxygen production, that mainly contribute to creating differences in $CBOD_5$ removal rates and the development of aerobic conditions. The model was also sensitive to atmospheric aeration rates at low temperature providing further evidence that low oxygen availability limits the treatment of $CBOD_5$ in cold climate WSPs. During the development process, it was discovered that common formulations of depth-integrated phytoplankton growth performed poorly for our modeled system, which was a quiescent eutrophic environment. This paper presents a new phytoplankton growth formula within the paradigm of a poorly-mixed eutrophic system that may find utilization in other eutrophic, colored or turbid systems. The novel aspect of the approach is that the depth integrated phytoplankton growth function was formulated upon the premise that the phytoplankton population would be capable to orient themselves to optimize their growth under poorly mixed conditions, and the average growth rate of the phytoplankton population must decrease as crowding puts pressure on shared resources. The general agreement of the model with the experiments, combined with the simplicity of the depth integrated box model, suggests there is potential for further development of the model as a tool for assessing proposed arctic WSP designs. The sensitivity analysis highlighted the uncertainty and importance of the parameterization of bacterial and phytoplankton physiology and metabolism in WSP models.

1 Introduction

Waste Stabilization Ponds (WSPs) are, in essence, shallow highly eutrophic water bodies used for municipal wastewater treatment, and operate by allowing biological (microbial degradation) and physical treatment processes (settling) to reduce the $CBOD_5$ (Carbonaceous Biochemical Oxygen Demand – Day 5) concentration prior to discharge from the treatment system. However, the design and operation of arctic WSPs is typically different than those used in warmer climates due to the prevailing cold temperatures, and short ice-free time periods. Arctic WSPs are operated as controlled discharge storage ponds; raw wastewater is continuously received into the WSP year round, but effluent is only discharged once per year, typically during late summer/early fall for a period of 2-3 weeks. The surfaces of the arctic WSPs stay frozen for 9-10 months and influent wastewater temperatures quickly approach 0 ˚C limiting the biological treatment capabilities of the system during this period. As a result, WSPs at the start of the summer treatment season, or ice free period, contain high concentrations of oxygen demanding substances ($CBOD_5$ >200 mg/l). The level of $CBOD_5$ treatment during the summer season is highly variable

(Ragush et al. 2017), and the limitations and best operational practices of single-cell WSPs operating in arctic environments have not been deeply investigated.

The current design guidelines and "best practices" that are presently in use in the Arctic were developed from the performance of systems operating in northern climates and expert experience (Dawson & Grainge, 1969; Heinke et al., 1991). However, these design guidelines were meant to meet less stringent effluent regulations (Nunavut Water Board, 2015) than are currently being implemented across Canada (Government of Canada, 2012). Also, the systems used to develop the guidelines were generally i) located in cold temperate (such as northern interior United States or Canada) or sub-arctic climates and/or were ii) continuous flow systems (US EPA, 1983). Since most northern communities (e.g. 19 of 25 in Nunavut, Canada) depend on WSPs as a component of their municipal wastewater treatment, the applicability of such guidelines for the design of arctic WSPs warrants further scrutiny.

To better understand the climatic and operational factors influencing the performance of single cell WSPs in cold climates, Ragush et al. (2017) used a bench-scale factorial design experiment to examine the influences of temperature, irradiance, organic loading and initial carbon concentration conditions at the onset of summer. The focus was to observe how the aforementioned parameters impact the development of an aerobic environment and $CBOD_5$ treatment performance. In this experiment, mesocosms were constructed to represent Arctic WSPs operating for 40 days, which is roughly the length of the summer treatment season in many Nunavut, Canada communities. Statistical analysis by Ragush et al. (2017) found that all four factors significantly impacted the oxygen state and $CBOD_5$ removal rates.

Here, a mechanistic model is presented with the intent to represent the carbon and oxygen dynamics in arctic WSPs. This model is to be used to explore existing knowledge gaps and uncertainties with respect to the dynamics occurring in these systems and to determining limiting factors of system performance. Ultimately, the model can be developed into a tool to assess arctic WSP design and optimization. With the focus of this study being on the mechanisms of $CBOD_5$ removal and oxygen concentration dynamics, the model needed to adequately represent the length of time required for algae populations to reach levels necessary to produce an aerobic (> 2 mg/L dissolved oxygen) environment under arctic temperature and light conditions. One of the ultimate objectives of this work was to identify organic loading regimes for arctic WSPs that facilitate the formation of aerobic environments within the relatively short (approximately 40 - 60 days) summer treatment season. During the development of this model, it

was found that formulations from the literature poorly represented phytoplankton growth in our stagnant eutrophic environment with high light attenuation. Thus, a mathematical representation for phytoplankton growth under these particular conditions was developed. Here, we present this new phytoplankton growth model, for environments that are eutrophic and have high light attenuation, which is likely to be applicable and have merit for simulations of other ecosystems where phytoplankton are space limited due to a small vertical window in optimal photic depth. Incorporating the new phytoplankton growth representation, we present a process-based model to predict dissolved oxygen and $CBOD_5$ concentrations in WSPs and provide an assessment of the local sensitivity of associated parameters of such a model through a one-factor-at-a-time (OFAT) sensitivity analysis. A brief discussion of simulation results of the sensitivity analysis is provided in the context of WSP design. The formulation of the model, specifically the depth-integrated phytoplankton growth function, and the results of the sensitivity analysis are likely to be adaptable to other eutrophic systems.

2 Model Development

The use of process-based models to design and evaluate wastewater treatment processes, specifically activated sludge systems, is well established (Orhon & Artan, 1994; Henze et al. 2000), and principles from these systems have also been coupled with ecosystem models and applied to WSPs (e.g. Gehring et al., 2010; Fritz et al., 1979; Buhr & Miller, 1983; Moreno-Grau et al., 1996; Banks et al., 2003; Beran & Kargi, 2005). These models display a large range in complexity and formulations depending upon the studies' objectives and design characteristics of the system. We reviewed the literature, assessing models for their applicability to our system and our focus on the prediction of dissolved oxygen concentration and $CBOD_5$ removal in WSPs operating in arctic environments. Banks et al. (2003), an adaptation of Buhr & Miller (1983), presented a box model of the photic zone (i.e. vertical surface region where there is sufficient light for photosynthesis) that forms the cornerstone of the model presented in this paper. However, when Banks et al.'s formulation was applied to the bench-scale system presented in Ragush et al. (2017) we found that it was unable to adequately predict the oxygen state and $CBOD_5$ concentration. The concentrations of oxygen, timing of when oxygen rose, and $CBOD_5$ removal could not be calibrated/validated between the entire set of experiments. The poor agreement is believed to be due to the fact that the Buhr & Miller (1983) system was a high-rate algal pond, which is shallow and has a paddle system engineered to create continually

well-mixed conditions. This is inconsistent with single cell WSPs operating in the Arctic that have greater depth and limited mixing. Thus, we made several modifications to the Buhr & Miller (1983) model.

2.1 Model overview

Figure 1 provides a schematic of the model along with references to the equations in Table 1 that were used to represent the major processes. It is stressed to the reader that the model is a heuristic representation of arctic WSPs, and accordingly is an abstraction of reality. This investigation uses the model to assess: i) the parameters that have the greatest impact on treatment performance and ii) the environmental conditions that are limiting the treatment performance in arctic WSPs, and the investigation does not aim to represent the model as an engineering design tool. Omissions of phytoplankton respiration and anaerobic processes were based on heuristics. Extended daylight during the summer in the North, allowing for continual photosynthesis, was the justification for the removal of phytoplankton respiration from the model, and the relative low activity of anaerobic processes when temperatures are less than 20 ˚C, as observed (Ragush et al. 2015; Ragush et al. 2017) in arctic WSPs, justified omission of anaerobic processes The model is a box model of the photic zone, and state variables and parameters were vertically-integrated over the depth of the photic zone. External forcing into the photic zone were additional wastewater, and surface irradiance. Exports from the photic zone were bacteria and phytoplankton through sinking. Gas exchange of oxygen and carbon dioxide between the atmosphere and photic zone was included as a transboundary interaction. Within the photic zone, the dynamics of bacteria and phytoplankton populations and their metabolites of oxygen, carbon dioxide, and carbon (in the form of $CBOD_5$) were modeled. Nutrients other than carbon, such as nitrogen and phosphorous, were excluded because their concentrations in both field scale and experimental WSPs are high, and it was assumed that they would not impact biological processes by being limiting (Ragush et al. 2015; Ragush et al. 2017).

The model formulation discussed in the following section will refer to equations by their number denoted in Tables 1 and 2 (for example Table 1 Equation 1 will be represented as equation 1.1 in the text). Table 1 contains the system of differential equations, while Table 2 contains the supporting equations. Table 3 provides a list of model parameters and their description. MATLAB, version R2015b, by MathWorks (Masschusetts, USA) was used to implement a numerical solution to the system of ordinary differential equations presented in Table 1. The system of ordinary differential equations is briefly discussed in section 2.1.1 and selected equations in Table 2 are discussed

where deemed appropriate following in section 2. Simulations were initialized using phytoplankton and bacteria concentrations that were reported by Ragush et al. (2017) at the beginning of their experiment.

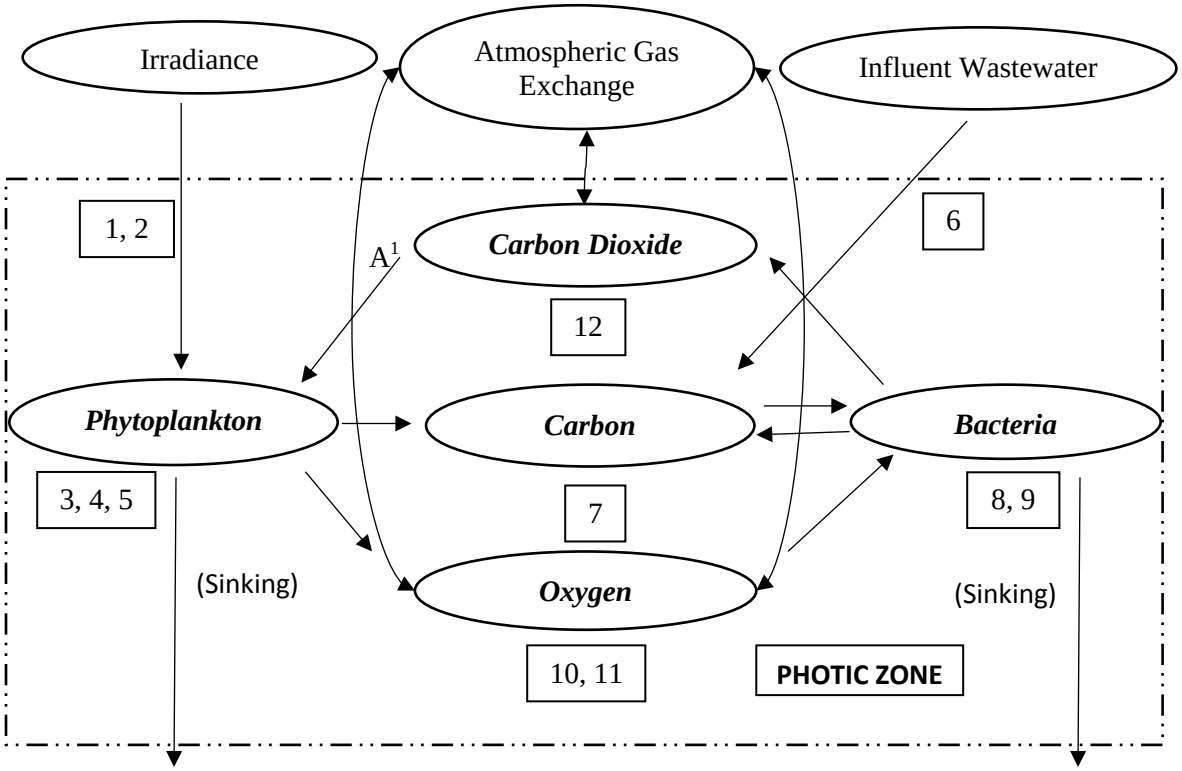

Figure 1 Diagram of modeled processes with listed applicable equations next to process arrows. A[1]Respiration of phytoplankton omitted because of net uptake of CO_2 and continual solar irradiance leads to the potential of uninterrupted photosynthesis. Bold and Italicized text denotes state variables.

Table 1 List of Ordinary Differential Equations (ODEs) with brief descriptions.

#	Equation	Description & Comments
1	$\frac{dA}{dT} = (U_a - K_{ad} - K_{as}) * A$	Rate of change in phytoplankton = (specific rates of Growth – death – settling) * phytoplankton density
2	$\frac{dS}{dT} = -(OUR) * B + L * \frac{CBOD5inf}{V} * \frac{ColumnZ}{Z} + K_{ad} * A * 0.5 + K_{db} * 0.7 * B$ Note S >= 0	Rate of change in $CBOD_5$ = consumption by bacteria + daily loading + inputs from phytoplankton death + inputs from bacteria death
3	$\frac{dB}{dt} = (U_B - K_{bd} - K_{bs})B$	Rate of Change in bacteria = (rates of growth – death – settling) * bacteria density
4	$\frac{dO_2}{dt} = Y_{oa} * U_a * A - (OUR) * B + Kl_{O_2} * \frac{Area}{V} * (Cs_{O_2} - O_2)$	Rate of Change of oxygen = Oxygenation by phytoplankton – Consumption by bacteria +aeration

5	$\frac{dCO_2}{dt} = \frac{Ycb}{Y_{ob}} * (OUR) * B - Y_{ca} * U_a * \mathrm{A} + Kl_{CO_2} * \frac{Area}{V} * \left(Cs_{CO_2} - CO_2\right)$	Rate of Change in carbon dioxide = production by bacteria – consumption by phytoplankton + aeration

147

148 *Table 2 List of supporting model equations and brief descriptions.*

#	Equation	Description & Comments
1	$Iav = Io\frac{1 - e^{\left(-(K_w + K_p * A) * z_{1\%}\right)}}{(K_w + K_p * A) * z_{1\%}}$	Average Irradiance across depth (considering shading by phytoplankton)
2	$z_{1\%} = \frac{\log(0.01)}{-K_w}$	Depth of 1% light transmittance (negating phytoplankton)
3	$Fdis = (1 - ED) * \left(1 - e^{-4e^{-(AGS)A}}\right) + ED$	Growth inhibition of phytoplankton as caused by crowding (Gompertz logistic growth model)
4	$U_a = Umax * F_{dis} * \frac{CO_2}{K_{CO_2} + CO_2} * \frac{Iav}{Iav + I_{halfsat}}$	Growth rate of phytoplankton = (Maximum phytoplankton growth rate * Crowding limitation * CO_2 limitation * Light Limitation)
5	$CBOD_{5inf}$ = RAW * SOL_{CBOD5}	Addition of $CBOD_5$ into photic zone = $CBOD_5$ concentration * solubility
6	$U_b = Umax_b * \frac{S}{K_s + S} * \frac{O_2}{K_{O_2} + O_2} * (1 - BGS * B)$	Growth rate of bacteria rate Maximum bacteria growth rate * carbon substrate limitation * Oxygen limitation * self-limitation (logistic growth)
7	If $dO_2 > OUR_b *$ $(OUR) = (OUR)_m * \frac{O_2}{O_2 * K_{O_2}} + (OUR)_b$ else $(OUR) = \frac{O_2}{B}$	Oxygen utilization rate: depends on the available oxygen and the bacterial population density
8	$CBOD_5(t)$ = S(t) + 0.5*(A(t))	$CBOD_5$ = Carbon pool $CBOD_5$ + $CBOD_5$ of phytoplankton ((t) denoting at time t for clarity)

149

150 *Table 3 List of model state variables and constants.*

Symbol	Definition	Value & Units
	State Variables	
A	Average phytoplankton concentration (algae)	mg/l (wet mass)
B	Bacteria concentration	mg/l (wet mass)
S	Substrate concentration (carbon)	mg/l ($CBOD_5$)
O_2	Oxygen concentration	mg/l
CO_2	Carbon dioxide concentration	mg/l
	Variables	
F_{dis}	Reduction in phytoplankton growth due to preferred distribution reducing irradiance	Unitless
I_{av}	Average irradiance across photic depth (Z) with phytoplankton	$\frac{\mu E}{m^2\, s}$

Constants		
$CBOD_{5inf}$	Influent CBOD5 concentration	550 mg/l
Z	Depth of water column (total depth)	1.25 m
Cs_{O2}	Saturation concentration oxygen	11.3 mg/l (5 ˚C) 8.9 mg/l (15 ˚C) NIST (2015)
Cs_{CO2}	Saturation concentration carbon dioxide	1.01 mg/l (5 ˚C) 0.75 mg/l (15 ˚C) Benson & Krause (1984)
L	Daily volumetric loading	0.0125 or 0.05 l/d
I_{av}	Average irradiance across photic depth (Z) with no phytoplankton	(Eqn 1) $\frac{\mu E}{m^2} s^{-1}$
I_o	Surface incident light	225 & 1050 $\frac{\mu E}{m^2} s^{-1}$
K_w	Attenuation coefficient of the wastewater	14 m^{-1}
SOL_{CBOD5}	Solubility Ratio of $CBOD_5$	0.5
V	Volume	0.0228 m^3
$z_{1\%}$	Photic zone depth (1% measured irradiance)	(Eqn 2) m

*Manually calibrated constants provided in Table 3

2.1.1 State Variables and Ordinary Differential Equations

The model has five state variables: phytoplankton, bacteria, carbon, oxygen, and carbon dioxide, and the first four were measured in the mesocosm study by Ragush et al. (2017), which were used to create a system of Ordinary Differential Equations represented in Table 1 and briefly discussed below:

$$\frac{dA}{dT} = (U_a - K_{ad} - K_{as}) * A \quad (1.1)$$

"A" represents phytoplankton (algae) as is used in many ecological models. The growth of phytoplankton population is the balance of its growth rate (U_a) with some loss rates separated into death (K_{ad}) and settling (K_{as}). The impact of death and settling has no mathematic functional difference and can be lumped with the same effect. They were separated here, as it is a common practice in ecological models.

$$\frac{dS}{dT} = -(OUR) * B + L * \frac{CBOD5inf}{V} * \frac{Z}{Z_{1\%}} + K_{ad} * A * 0.5 + K_{bd} * 0.7 * B \quad (1.2)$$

"S" commonly represents substrate in ecological models; here it represents $CBOD_5$. The substrate is consumed by the bacteria in a stochiometric balance of the bacteria's oxygen utilization rate (OUR). Additional $CBOD_5$ is added daily, as wastewater is added to the system, and CBOD5 is recycled in the death of phytoplankton (A) and bacteria (B) according to stochiometric carbon compositions.

$$\frac{dB}{dt} = (U_B - K_{bd} - K_{bs})B \quad (1.3)$$

"B", Bacteria is controlled analogously to phytoplankton with growth rate (U_b) , death rate (K_{bd}), and settling rate (K_{bs}).

$$\frac{dO_2}{dt} = Y_{oa} * U_a * A - (OUR) * B + Kl_{O_2} * \frac{Area}{V} * \left(Cs_{O_2} - O_2\right) \quad (1.4)$$

The differential equation for oxygen is governed by photosynthesis of phytoplankton, the utilization by bacteria and finally oxygen transfer rate across the quiescent surface.

$$\frac{dCO_2}{dt} = \frac{Y_{bc}}{Y_{bo}} * (OUR) * B - Y_{ac} * U_a * \mathrm{A} + Kl_{CO_2} * \frac{Area}{V} * \left(Cs_{CO_2} - CO_2\right) \quad (1.5)$$

Analogous to the equation for oxygen, the equation for carbon dioxide includes production from bacteria, uptake from phytoplankton and carbon dioxide transfer across the surface.

Graphs are provided to compare the experimental and modelling result in figures 3 and 4 for carbon (measured through $CBOD_5$) and dissolved oxygen, respectively. A graph of the phytoplankton and bacteria results are provided for the most interesting case scenario of 80 mg/l initial $CBOD_5$ and 15 ˚C environmental temperature in Figure S1 in the supplemental material. The model includes the state variable of carbon dioxide, however, no data was available to create a comparison for this state variable, as this parameter was not measured by Ragush et al. (2017). Carbon dioxide was included as a state variable because a state limitation was required to explain the decrease of phytoplankton and bacteria populations in the later stage of some trials (Supplemental 1). Typically, a light limitation would be expected to have caused the limit on population, however in this model with no mixing it would result in a steady state phytoplankton population, and this was not observed. Since the decrease in phytoplankton and bacteria populations coincided with the decrease in available organic carbon, it was hypothesized to be an organic carbon/carbon dioxide limitation. It is noteworthy that carbon dioxide limitation has been identified as a cause of phytoplankton population crashes in waste stabilization ponds **(**Shilton 2005**)**. The authors recognize the possibility that an alternative reason could be a micronutrient as the limiting agent, and the hypothesis that it is carbon dioxide warrants further investigation. However, the existence of a different limiting agent has negligible impact on the goals of this investigation and only a minor reformulation of the model would be required to accommodate this realization.

The authors recognize that this model simplifies the complex inorganic carbon dynamics and does not explicitly consider the potential uptake of other inorganic carbon species such as bicarbonate by phytoplankton. The data does

not exist to justify the incorporation of these complicating processes, and from a heuristic perspective their inclusion is outside the scope of the model. The authors see their inclusion as an avenue of investigation for future model improvements.

2.2 Temperature

The temperature dependences of chemical, physical and biological processes were modelled based on the van't Hoff-Arrhenius relationship (equation 2.1) from Metcalf & Eddy (2003) who used a range of 1.024 -1.08 for θ (equivalent to an approximate Q_{10} of 1.3-2.2) for biological processes. For the physical process of aeration Elmore and West (1961) suggests a value of 1.024 (equivalent). Due to lack of data, and to maintain simplicity and focus of the study, all temperature dependent processes were modelled with a θ of 1.024 except the phytoplankton maximum growth rate. The van't Hoff-Arrhenius relationship was not applied to phytoplankton maximum growth rate because literature supported a larger temperature dependence, and Dauta et al. (1990) estimated maximum phytoplankton growth rates of 0.3 day^{-1} at 5 ˚C and 0.72 day^{-1} at 15 ˚C: equivalent to a Q_{10} of 2.4. During our study, the phytoplankton growth rates were calibrated to 0.32 day^{-1} at and 0.75 day^{-1} at 5 ˚C and 15 ˚C; values remarkably close to those recorded by Dauta et al. (1990). The model was found to be insensitive to any change in the growth rate of bacteria in the range of literature values (Tables 5 & 6).

$$Rate_{Temperature} = Rate_{20C} * \theta^{(T-20)} \quad (2.1)$$

2.3 Phytoplankton

Modeling of phytoplankton populations and their growth must account for the vertical distribution of the population and the vertical gradients in irradiance, nutrients, and metabolites. As our system represents a special case of high light attenuation, limited vertical mixing forces, and high nutrients, phytoplankton growth was formulated on the premise that the phytoplankton population has the ability to optimize its growth rate and will distribute itself accordingly. The formulation is significantly different than common formulations used for well-mixed environments such as in Huisman and Weissing (1994). The deviation was out of a necessity as it was discovered that the unique environmental conditions required approaching the problem from a different paradigm. Sections 2.3 focuses on the process by which the novel formulation for phytoplankton growth was developed to describe the arctic WSP. The development of the mathematical characterization of the depth integrated phytoplankton response for a WSP

219 requires careful consideration of three factors: i) phytoplankton-light response ii) population density limited growth,
220 and iii) photoinhibition.

221 2.3.1 Phytoplankton light response

222 Solar radiation provides the energy for photosynthesis, and the total (vertically integrated) phytoplankton production
223 will be proportional to the amount of energy absorbed by the phytoplankton. Not all of the irradiance that reaches
224 the surface of the water column can be utilized by the phytoplankton because light energy is also absorbed or
225 reflected by particles. Additionally, light photons are absorbed by the phytoplankton cells themselves, reducing the
226 available irradiance to other cells (specifically at greater depth) and as the vertically integrated population density
227 increases the available irradiance per individual must decrease, and is known as self-shading. Finally, the response
228 of the depth-integrated phytoplankton population in the photic zone is assumed to be related to the average
229 irradiance in the photic zone by a hyperbolic function.

230 The transmittance of light has been demonstrated to be successfully approximated to follow exponential decay with
231 distance through a media, and is commonly described by Beer-Lambert's law:

$$I_z = I_o e^{-kz}$$

232 Where: I_o = irradiance at surface (depth 0 m), I_z = irradiance at depth z ($\mu E/m^2/s$), k = attenuation coefficient (m^{-1}),
233 and z = depth (m)

234 The attenuation coefficient is a water quality property i.e. an expression of color and suspended solids (Lorenzen
235 1972)**.** When modeling vertically varying phytoplankton growth, it is common to define the euphotic zone depth, as
236 the depth where 1% of the surface light may be measured in a water column with attenuation properties of k:

237 $$-\frac{Ln(0.01)}{k} = z_{1\%} \quad (2.2)\ (\text{Lorenzen 1972})$$

238 Phytoplankton concentrations change with depth and time, and therefore k was split into two contributors; k_w
239 (considered a property of the water and its constituents), and k_p (accounts for the absorption of light by
240 phytoplankton).

241 $$k = k_w + k_p(\text{A(t)})\ (\text{Lorenzen 1972})$$

Where: k_w = Light attenuation coefficient of water and constituents (m^{-1}), k_p = Light attenuation coefficient of phytoplankton (m^{-1}/ [mg/l]), and A = phytoplankton concentration (mg/l)

k_w and k_p were considered homogenous and constant over the duration of the simulation.

The average light in the photic zone (between the surface and $Z_{1\%}$) can be approximated by incorporating attenuation into Beer-Lambert's law and integrating over the photic zone and averaging over the depth:

$$Iav = \frac{1}{z_{1\%}} \int_0^{z_{1\%}} I_o e^{-kz} = \frac{1-e^{-(k_w+p*A)(Z_{1\%})}}{(k_w+k_p*A)z_{1\%}} \quad (2.1)$$

Note that in this formulation of the production-irradiance relationship average irradiance and phytoplankton values are used, and results in an average growth rate in the photic zone. Although neither the phytoplankton concentration nor the irradiance is constant with depth, an appropriately parameterized box model is not compromised by using the average values; however, the parameterization is likely to be impacted (Behrenfeld & Falkowski 1997). The average irradiance in the photic zone was used in the Michaelis-Menten equation for the production-irradiance response of phytoplankton (Equation 4) with the half saturation constant of *Chlorella vulgaris* as reported by Dauta et al. (1990). Alternatively, it was found that the exponential formulation for the phytoplankton-irradiance curve ($1-\exp(-\alpha I_{av}/U_{max})$) can be substituted with a value of 0.016 for α/Umax (assumed constant with temperature) with no impact on model results.

2.3.2 Phytoplankton Distribution

If light was the only controlling factor of phytoplankton growth, it would be optimal for phytoplankton to grow in large concentrations over a narrow depth where irradiance was optimal. Although phytoplankton populations predictably reside in greatest concentrations near the depth of optimal irradiance (assuming no nutrient limitations) (Mellard et al. 2011), as the population grows the vertical range inhabited expands out from the area of optimal irradiance (Klausmeier and Litchman 2001). The physiological causes for this broadening of the vertical population structure were not identified in this study, however the authors postulate that it is biological stressors related to limitations in extracellular mass transfer rates (diffusion) of metabolites, such as carbon dioxide, oxygen, and nutrients that create this vertical distribution. We assume phytoplankton can only obtain their maximum growth rate at low population densities, when nutrients and light are abundant and the stressors associated with high population

densities are not present. We propose that the impact of self-limitation of phytoplankton growth is a critical element in modeling phytoplankton dynamics in nutrient rich systems with minimal vertical mixing. Populations that experience self-limitation with density are commonly described with logistic growth models, and in our model we utilized a generalized logistic growth model, the Gompertz model (F_{dis}). The Gompertz model has been utilized extensively in the modelling of bacteria populations (Contois, 1959, Zwietering et al. 1990), however the function is difficult to visualize, and so a plot of F_{dis} (Figure 2) has been provided to clearly depict the response of this function and demonstrate how it represents the aforementioned goals**.** The parameters of F_{Dis}, AGS (Phytoplankton Growth Self-suppression) and ED (Equal Distribution), can be estimated through review of literature, however AGS and ED were largely used in calibration of the model because more experimentation of the relationship between phytoplankton density and phytoplankton growth is needed. The resulting formulation is:

$$\mathrm{Fdis} = (1 - \mathrm{ED}) * \left(1 - \mathrm{e}^{-4\mathrm{e}^{-(\mathrm{AGS})\mathrm{A}}}\right) + \mathrm{ED} \quad (2.3)$$

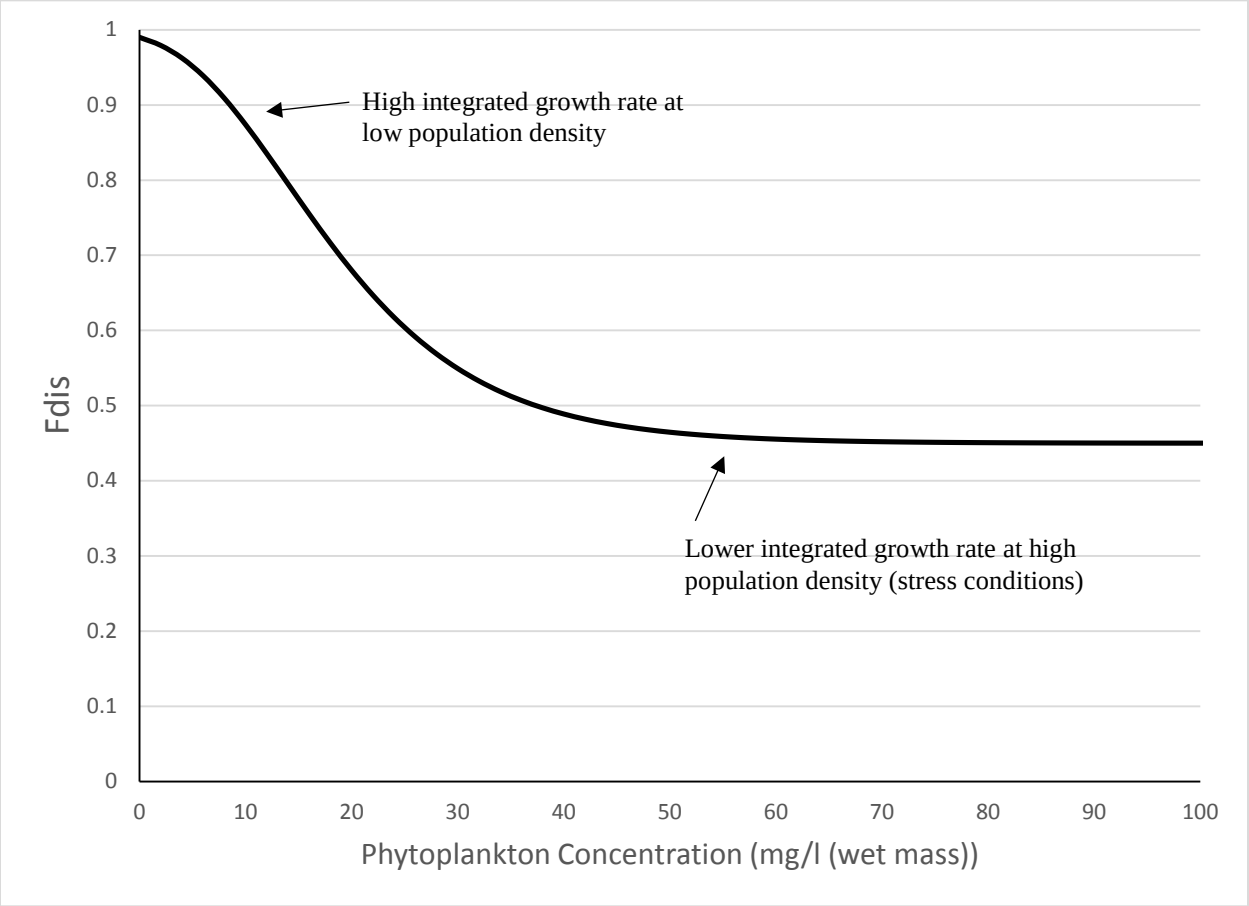

Figure 2. Representation of the changes in integrated phytoplankton growth rate (Fdis) with increasing phytoplankton concentration.

2.3.2.1 Photoinhibition

The growth rate of phytoplankton increases with increasing irradiance until an optimal irradiance results in a maximum growth rate, after which a decline in growth rate is typically observed (Dauta et al., 1990). The observation of such as photoinhibition has been documented in small batch reactors where phytoplankton are confined and subjected to high irradiance. However, photoinhibition is the result of a phytoplankton's inability to remove the stressor of excessive irradiance and UV radiation forming harmful reactive oxygen species, and it can be rationalized that provided the phytoplankton has adequate (i) space and (ii) mobility, they will avoid photoinhibition by migrating towards lower-light levels where their growth is optimized. This would result in a threshold irradiance where, the vertically integrated specific growth rate has reached a satiated maximum and is an implicit

representation of photoinhibition. The authors note that the exclusion of explicit photoinhibition is specific to a case where currents or mixing do not overwhelm the phytoplankton's mobility and the growth of phytoplankton is integrated over a control depth.

2.4 Bacteria

A logistic growth model (Equation 8), with a death term was used to describe heterotrophic bacteria growth. Bacterial growth suppression (BGS) is approximately the inverse of the carrying capacity, as BGS multiplied by the maximum bacteria population will provide a value of 1, resulting in bacterial growth rate of zero. The aerobic metabolism was based on an oxygen utilization rate (OUR) (units of mg O_2/ mg bacteria day^{-1}) that consisted of the basal oxygen utilization rate (our_b) required to sustain the existing population, and an additional oxygen utilization rate (our_m) required for the population to grow (Equation 10). It was reasoned that in the case there was less oxygen available than desired by the bacteria, the bacteria would use all the oxygen (resulting in an OUR equal to the available oxygen concentration divided amongst the bacteria concentration). The model does not consider the potential for anaerobic growth of bacteria. The removal of $CBOD_5$ was equivalent to the amount of oxygen used, and the production of CO_2 was computed based on the stoichiometry of carbon dioxide produced for every unit of oxygen used (Y_{bc}/Y_{bo}).

2.5 Carbon Cycling

Phytoplankton and bacteria return carbon back into the organic pool upon death (Equation 7). From literature, it was estimated that 1 mg of dry phytoplankton mass has a chemical oxygen demand (COD) of 1 mg (Boyd 1973) and The general relationship of 1 mg/l $CBOD_5$: 2 mg/l COD was used resulting in 0.5 mg $CBOD_5$/mg phytoplankton and 0.7 mg $CBOD_5$/mg bacteria. Additionally, the $CBOD_5$ of the phytoplankton was also accounted for in equation 13 by adding the $CBOD_5$ of the phytoplankton to the $CBOD_5$ of the organic pool. Bacteria was omitted from being considered in the $CBOD_5$ pool because it forms the community that is responsible for the utilization of oxygen within the $CBOD_5$ test and therefore cannot be enumerated.

3 Results and Discussion

The model was used to investigate the experimental results from Ragush et al. (2017). In the experiment, mesocosms representative of arctic WSPs were constructed to assess the impact of temperature, irradiance, organic loading rate, and initial organic concentration. The experiment was run either until steady state of oxygen and $CBOD_5$ were achieved or for 40 days. The populations of phytoplankton and bacteria, and $CBOD_5$ concentration were measured every 5-7 days while dissolved oxygen concentration was measured daily. The system was operated in a manner that is analogous to systems in the North, with daily loading of carbon and nutrients being imitated with a complex synthetic wastewater. Temperature and irradiance were maintained as constants for the duration of trials. The water level was maintained through the addition of distilled water to replace evaporated volume to remove the impact of any concentrating effect.

3.1 Model Calibration and Performance

Experimental results from Ragush et al. (2017) were used to calibrate the model. The calibration was performed by fitting the model to the experimental results of $CBOD_5$ and dissolved oxygen concentrations obtained at 5˚C, and then validating against experimental results generated at 15 ˚C. Maximum phytoplankton growth rates ($Umax_a$) were set to the values provided by Dauta et al. (1990). $Umax_a$ was then calibrated at both temperatures, however, the calibration values (0.32 and 0.75 $days^{-1}$ at 5 and 15 °C, respectively) represented only a minor adjustment from growth rates (0.3 and 0.7 $days^{-1}$) provided by Dauta et al. (2010). The model was calibrated at both temperatures with a 240 mg/l initial carbon concentration, and validated at 80 mg/l initial carbon concentration. The values of the calibrated parameters are provided in Table 4. Figures 3 and 4 depict the model predicted (lines) and experimental observed (symbols) $CBOD_5$ and dissolved oxygen concentrations, respectively, under the different temperature and initial loading conditions and show that the model is able to capture the general trends and effectively distinguishes system dynamics for the various conditions. Such qualitative model-data comparison is sufficient for the purposes of this paper, which focuses on exploration of the parameterization and impact of different environmental conditions.

Table 4. Manually calibrated model parameters.

Parameter	Definition	Units	Value
Ihalfsat	Irradiance half saturation of phytoplankton	$\frac{\mu E}{m^2} s^{-1}$	30

K_{ad}	Phytoplankton death rate	day^{-1}	0.05
K_{as}	Phytoplankton settling	day^{-1}	0.05
K_{bd}	Bacteria death rate	day^{-1}	0.025
K_{bs}	Bacteria settling	day^{-1}	0
K_{CO2}	Half saturation of phytoplankton on carbon dioxide	$\frac{mg\ CO_2}{l}$	0.044
K_{O2}	Half saturation of bacteria on oxygen	$\frac{mg\ O_2}{l}$	0.256
K_p	Light abstraction by phytoplankton	$\frac{m^{-1}}{mg/l}$	0.13
Kl_{CO2}	Carbon Dioxide transfer rate (piston velocity)	$\frac{m}{day}$	0.17 (@ 20 ˚C)
Kl_{O2}	Oxygen transfer rate (piston velocity)	$\frac{m}{day}$	0.17 (@ 20 ˚C)
Ks	Half saturation of bacteria on substrate	$\frac{mg\ CBOD_5}{l}$	80
our_b	Basal oxygen utilization rate of bacteria	$\frac{mg\ O_2}{mg\ bac} day^{-1}$	0.10 (@ 20 ˚C)
our_m	Metabolic oxygen utilization rate of bacteria	$\frac{mg\ O_2}{mg\ bac} day^{-1}$	0.55 (@ 20 ˚C)
$Umax_a$	Max growth rate phytoplankton	day^{-1}	0.75 (@ 15 ˚C) 0.32 (@ 5 ˚C)
$Umax_b$	Max growth rate bacteria	day^{-1}	5
Yac	Yield factor of CO_2 consumed per a mg of phytoplankton	$\frac{mg\ CO_2}{mg\ Phytoplankton}$	2.18
Y_{bc}/Y_{bo}	Carbon dioxide/ oxygen produced	mg CO_2 / mg O_2	1.38
BGS	Bacterial Growth Self Suppression	l/mg	0.01
AGS	Phytoplankton growth Self suppression	Unitless	0.1
ED	Equal Distribution Factor	Unitless	0.45

341

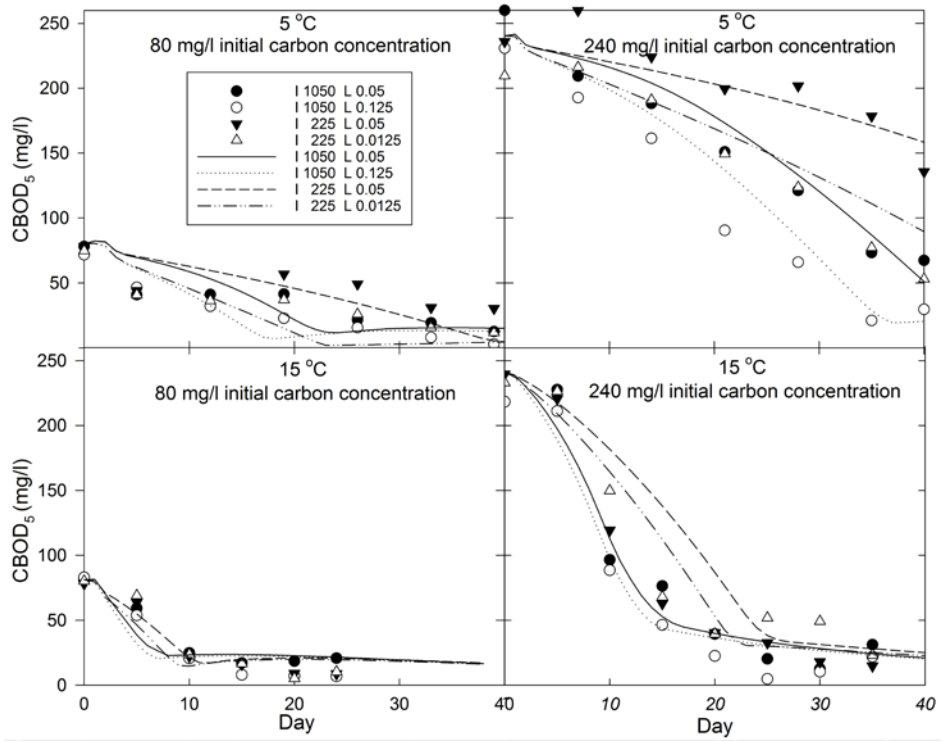

342

343 *Figure 3. Concentrations of CBOD5 in model waste stabilization ponds operating at 5 or 15°C with different initial carbon*
344 *concentrations (80 or 240 mg/l). The model performance for CBOD5 concentration predictions under the different conditions is*
345 *shown as lines, while the experimental results from Ragush et al. (2017) are shown as symbols. I denotes the modelled and*
346 *experimental irradiance ($\mu E/m^2/s$) and L is the volumetric loading rate (m^3/day),*

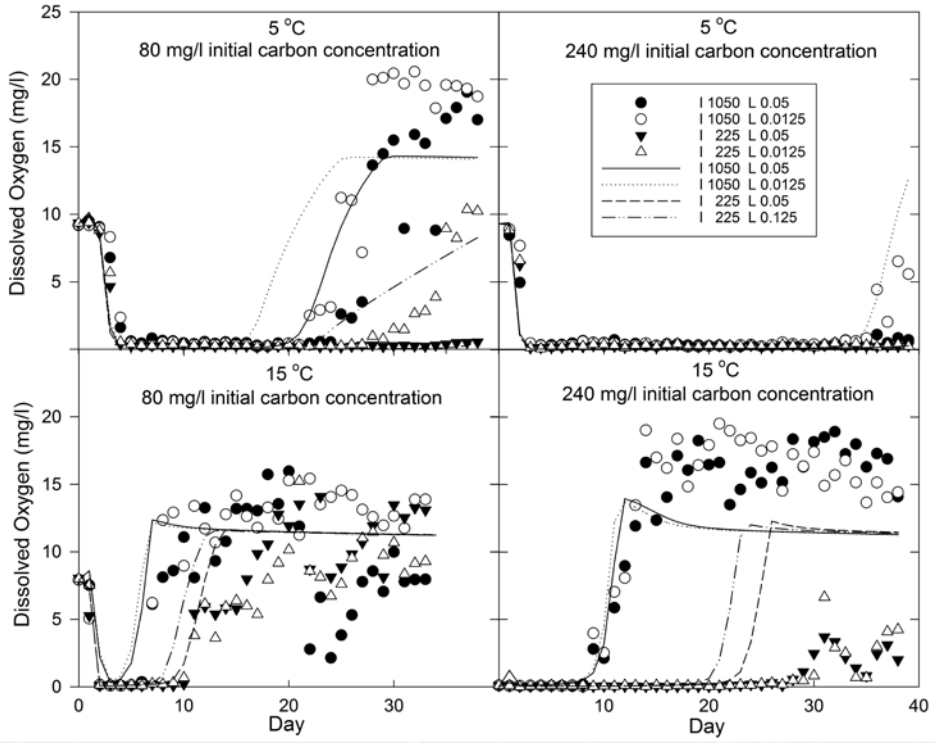

Figure 4. Dissolved oxygen concentrations in model waste stabilization ponds operating at 5 or 15°C with different initial carbon concentrations (80 or 240 mg/l).The model performance for dissolved oxygen concentration predictions under the different experimental conditions are shown as line, while the experimental results from Ragush et al. (2017) are shown as symbols. I is the modelled and experimenal irradiance ($\mu E/m^2/s$) and L is the volumetric loading rate (m^3/day),

While in general, good qualitative agreement between model and experimental results was observed, several inconsistencies provide insight into areas that are not well represented by the model and require further research. For example, the model underestimated the maximum dissolved oxygen concentrations (as measured at the surface), and predicted the development of measurable oxygen concentrations (> 0.5 mg/l) earlier than was found experimentally (Figure 4). The model's prediction of lower maximum oxygen may be due to differences between what is modeled versus measured. Specifically, the model represents average concentrations over the photic zone, whereas measured values were taken at a depth where oxygen was likely at its maximum. To determine if it is a discrepancy between what is being measured vs modeled, increased measurement resolution by placing sensors throughout the photic zone would be necessary. The model's tendency to predict measureable oxygen concentration earlier than experimentally observed, especially under low light conditions, may be due to neglecting O_2 diffusion from the oxygen productive photic zone deeper into aphotic (anoxic) zone. Furthering this thought concerning the model's late prediction of measurable oxygen concentrations appearing as seen in Figure 4, the flux of oxygen from the photic to aphotic zone early in the experiment is of a similar magnitude to that of oxygen production of

phytoplankton in the early stages of phytoplankton growth. As phytoplankton populations increase the impact of molecular diffusion on the oxygen concentration decreases relative to other factors such as oxygen production by phytoplankton.

The model only considers aerobic metabolism of bacteria for the removal of $CBOD_5$, and due to the good agreement with experimental results, this appears to be a reasonable simplification. However, when hypoxic conditions prevail, especially under low light conditions with minimal oxygen production by photosynthesis, the model under-predicts the treatment performance (Figure 3). The incorporation of anaerobic processes is likely to improve the robustness and prediction under low light and cold conditions.

Finally, from a practical application, the model was able to capture the influence of organic loading rates and initial carbon concentrations on dissolved oxygen and $CBOD_5$ concentrations (Figures 3 and 4). These are two key parameters that WSP designers are able to control. Such findings suggest arctic WSPs can obtain an effluent concentration for $CBOD_5$ that meet secondary wastewater treatment standards (25 mg/l) with lowered areal loading rates, and more importantly lowered carbon concentrations at the onset of the summer treatment season.

3.2 Sensitivity Analysis

A one-factor-at-a-time (OFAT) method local sensitivity analysis (or nominal range analysis) was performed post calibration of the model. An OFAT does not assess the parameter interactions and results of the OFAT may be impacted by the values of other parameters set during the calibration. The sensitivity analysis was carried out on the 20 parameters in Table 1. The parameter range tested was chosen based upon values reported in the literature, listed in Table 4. OFAT is an effective way of determining the model parameters that carry the most influence on output results (Cullen and Frey 1999), and is useful for identifying where to focus data collection related to improving the model (Salehi et al. 2000). These two strengths are directly in-line with the exploratory goals of this paper. In the OFAT, parameters were set to the calibrated value (Table 4) and one parameter at a time was varied over 5 equally-spaced levels that ranged between the high and low values reported in the literature when available (Table 5) or else a range of (+/- 25%).

Table 5 Parameter values from literature

Parameter	Definition	Units	Reported Values	Sources

Ihalfsat	Irradiance half saturation of phytoplankton	$\frac{\mu E}{m^2} s^{-1}$	30 60 220	Dauta et al. (1990) Moreno-Grau et al. (1996) Beran & Kargi (2005)
K_{ad}	Phytoplankton death rate	day^{-1}	0.05 0.001 0.05-0.25	Lawrence & McCarty (1970) Moreno-Grau et al. (1996) Schnoor (1996)
K_{as}	Phytoplankton settling/respiration	day^{-1}	0.2 m/d 0.05	Schnoor (1996) Moreno-Grau et al. (1996)
K_{bd}	Bacteria death rate	day^{-1}	0.035 0.1 0.06 death 0.06-0.015	Moreno-Grau et al. (1996) Buhr & Miller (1983) Beran (2005) Metcalf & Eddy (2003)
K_{bs}	Bacteria respiration/settling rate	day^{-1}	0.085 (+/- 25%)	Moreno-Grau (1996)
K_{CO2}	Half saturation of phytoplankton on carbon dioxide	$\frac{mg\ CO_2}{l}$	0.044 (+/- 25%)	Buhr & Miller (1983)
K_{O2}	Half saturation of bacteria on oxygen	$\frac{mg\ O_2}{l}$	0.256 0.128 1	Buhr & Miller 1983 Banks et al. (2003) Tchobanoglous et al. (2003)
K_p	Light abstraction by phytoplankton	$\frac{m^{-1}}{mg/l}$	0.138 – 0.0249	Lorenzen (1972) Li (2009)
K_s	Half saturation of bacteria on substrate	$\frac{m}{day}$	25-100 (60) 150	Metcalf & Eddy (2003) Lawrence & McCarty (1970)
Kl_{CO2}	Carbon Dioxide transfer rate (piston velocity)	$\frac{m}{day}$	0.893 1	Boogerd et al. (1989) Schnoor (1996)
Kl_{O2}	Oxygen transfer rate (piston velocity)	$\frac{mg\ CBOD_5}{l}$	0.15 0.189 0.24	Schnoor (1996) Chu & Jirka (2003) Deacon (1977)
our_b	Basal oxygen utilization rate of bacteria	$\frac{mg\ O_2}{mg\ bac} day^{-1}$	0.15 (+/- 25%)	Jenkins (1978)
our_m	Metabolic oxygen utilization rate of bacteria	$\frac{mg\ O_2}{mg\ bac} day^{-1}$	0.85 (+/- 25%)	Jenkins (1978)
$Umax_a$	Max growth rate phytoplankton	day^{-1}	0.3 (5 ˚C) 0.7 (15 ˚C) 0.5 0.48 (5 ˚C) 0.78 (15 ˚C) 1.13 (@20 ˚C) 1.5 (@20 ˚C)	Dauta et al. (1990) Moreno-Grau et al. (1996) Buhr & Miller (1983) Banks (2003) Schoor (1996)
$Umax_b$	Max growth rate bacteria	day^{-1}	4.95 5.0 2-10	Banks (2003) Moreno-Grau et al. (1996) Metcalf & Eddy (2003)
Y_{ca}	Yield factor of phytoplankton produced for CO_2 consumed	$\frac{mg\ CO_2}{mg\ Phyplankton}$	2.18 1.83 1.82	Fogg (1953) Cramer &Myers (1948) McKinney (2004)

Y_{Ca}/Y_{oa}	Carbon dioxide/ oxygen produced	mg CO_2 / mg O_2	1.25 – 1.37	Fogg (1953) Cramer & Myers (1948) McKinney (2004)
BGS	Bacterial Growth Self Suppression	mg/l $^{-1}$	0.002– 0.05	Estimated
AGS	Phytoplankton growth Self suppression	Unitless	0.02 – 0.5	Estimated
ED	Equal Distribution	Unitless	0.25 – 0.6	Estimated

Sensitivity coefficients (SC) were developed for two chemical responses, i.e., when dissolved oxygen first exceeds 2 mg/l, and when $CBOD_5$ concentrations are reduced to 30 mg/l and four biological response metrics, i.e., the timing of and maximum predicted phytoplankton and bacteria populations. The sensitivity coefficient provides a non-dimensional measure of relative influence of parameters to the relative change in the response (Downing et al. 1985). The sensitivity coefficient was calculated according to Equation 3.1, and five parameter values (the original and two higher and two lower) were used to determine an average SC over the parameter range (equation 3.2). The SC was taken to be the average to smooth out non-linearities within the relationship. Sensitivity analysis was performed at both lighting and temperature conditions at an initial carbon concentration of 240 mg/l and 0.0125 l/d loading rate to examine if the sensitivity of the parameters varied with environmental conditions. Tables 6 and 7 list the sensitivity coefficients for timing of dissolved oxygen concentration exceeding 2 mg/l and timing of $CBOD_5$ concentration below 30 mg/l. Insights from Table 5 and 6 will be discussed further in this section.

$$SC(P)_i = \left|\frac{dR}{dP_i}\right|_{P^0} = \frac{\frac{R_i - R_o}{R_o}}{\frac{P_i - P_o}{P_o}} \quad (3.1)$$

Where:
R = response vector, P = parameter vector, SC(P) = Sensitivity Coefficient of parameter p, and O = origin of parameter value (middle value of range tested)

$$SC(P) = \frac{\sum_i^n SC(P)_i}{n} \quad (3.2)$$

Table 6. Parameter sensitivity coefficient for timing of dissolved oxygen concentration exceeding 2 mg/l. Parameters with higher values are more sensitive.

Temperature (˚C)	**5**	**15**	**5**	**15**
Light (µE/m^2/s)	**250**	**250**	**1000**	**1000**
Ihalfsat	**0.41**	**0.47**	**0.49**	**0.67**

K_{ad}	**0.54**	**0.38**	**0.77**	**0.45**
K_{as}	**0.11**	**0.14**	**0.16**	**0.13**
K_{bs}	0.03	0.01	0.02	0.01
K_{bd}	**0.70**	**0.17**	**0.31**	0.03
K_s	0.02	**0.10**	0.06	**0.17**
K_{O2}	0.00	0.04	0.02	0.09
K_C	0.00	0.01	0.00	0.01
K_p	0.03	**0.10**	0.02	0.04
Kl_{CO2}	0.00	0.00	0.00	0.00
Kl_{O2}	**0.73**	**0.26**	**0.47**	**0.14**
our_b	0.01	0.08	0.04	**0.15**
our_m	0.03	0.05	0.01	**0.19**
$Umax_a$	**0.98**	**1.46**	**1.32**	**1.74**
$Umax_b$	0.03	0.01	0.02	0.01
Yca	**0.55**	**0.66**	**0.65**	**0.61**
YcaOYca	**0.56**	**0.68**	**0.66**	**0.68**
BGS	**0.82**	**1.50**	**1.45**	**2.60**
AGS	**0.34**	**0.33**	**0.40**	**0.21**
ED	**0.15**	**0.57**	**0.37**	**0.74**

410

411

412 *Table 7. Parameter sensitivity coefficients for timing of CBOD5 concentration below 30 mg/l*

Temperature (˚C)	**5**	**15**	**5**	**15**
Light (µE/m^2/s)	**250**	**250**	**1000**	**1000**
Ihalfsat	**0.29**	**0.86**	**0.46**	**0.47**
K_{ad}	**0.48**	**0.31**	**0.54**	**0.25**
K_{as}	**0.10**	0.09	**0.11**	0.04
K_{bs}	0.02	0.00	0.01	0.01
K_{bd}	**0.73**	**0.26**	**0.36**	**0.20**
K_s	0.00	0.03	0.01	**0.15**
K_{O2}	0.01	0.02	0.01	0.03
K_{CO2}	0.00	0.01	0.00	0.01
K_p	0.03	0.06	0.02	0.01
Kl_{CO2}	0.00	0.00	0.00	0.00
Kl_{O2}	**0.71**	**0.26**	**0.47**	**0.13**
our_b	**0.13**	0.03	0.05	**0.10**
our_m	0.04	0.02	0.03	**0.11**
$Umax_a$	**0.88**	**1.10**	**1.18**	**0.85**
$Umax_b$	0.03	0.00	0.01	0.02

Yca	**0.50**	**0.57**	**0.60**	**0.41**
YcaOYca	**0.51**	**0.58**	**0.59**	**0.43**
BGS	**0.23**	**0.68**	0.03	**0.91**
AGS	**0.29**	**0.28**	**0.41**	**0.34**
ED	**0.12**	**0.39**	**0.27**	**0.32**

A cumulative sensitivity report was constructed to provide a qualitative assessment of parameter sensitivity across the range of temperature and irradiance conditions, and a measure of relative parameter sensitivity in the model. Table 7 provides a sensitivity index by tallying the number of sensitivity coefficients of the 6 tested responses that exceeded 0.1 (a value that was arbitrarily assigned as being an indicator of a sensitive parameter) for a parameter under the noted temperature and irradiance conditions. To provide a comparison of parameter sensitivity, the right column total is a summation of exceedances for a parameter under all temperature/light conditions, and sensitivity ranking of the parameters developed by blending the response sensitivity coefficients. Finally, to compare sensitivity of the model under the four light/temperature pairings, a summation of the sensitivity index for each pairing is provided in the bottom row of Table 7.

Table 8 Cumulative sensitivity index by parameter or temperature/irradiance. Value denotes number of SI indices greater than 0.1 for 6 tested categories (see Tables 6 and 7).

Temperature (˚C)	**5**	**15**	**5**	**15**		**Sensitivity**
Irradiance (ue/m^2/s)	**225**	**225**	**1025**	**1025**	**Total**	**Ranking**
Ihalfsat	4	6	5	5	20	2
K_{ad}	4	5	6	5	20	5
Kas	5	3	5	2	15	12
Kbs	2	0	0	0	2	15
Kbd	5	5	5	3	2	9
K_s	0	1	0	3	4	14
K_{O2}	0	0	0	0	0	18
K_{CO2}	0	0	0	0	0	20
K_p	0	1	0	0	1	16
Kl_{CO2}	0	0	0	1	1	19
Kl_{O2}	4	5	5	4	18	10
our_b	3	3	4	3	13	11
our_m	1	0	0	4	5	13
Umaxa	6	5	5	5	21	1
Umaxb	0	0	0	0	0	17
Yca	6	5	5	5	21	4
YcaOYco	5	5	5	5	20	6

BGS	5	5	5	6	21	3
AGS	6	5	5	4	20	8
EDFactor	4	5	5	5	19	7
Total	60	59	60	60		

425

426 Parameter sensitivity was consistent for all the tested irradiance and temperature conditions (Table 7). However, the
427 sensitivity of certain parameters, such as oxygen aeration rate (Kl_{O2}) and bacterial growth self-suppression (BGS)
428 can vary greatly with changing environmental conditions (Tables 5 and 6). Finally, the analysis highlighted the
429 model's sensitivity to phytoplankton growth parameters as six of the seven most sensitive parameters are related to
430 phytoplankton growth rate or metabolism (Table 7).

431 Critical assessment of the sensitivity analysis provides insight into model dynamics and limiting processes under
432 different conditions. In general, the tested model was more impacted by changing parameter values at lower
433 temperature, and this result reinforces findings that the $CBOD_5$ removal and oxygen dynamics in the WSP are less
434 stable at lower temperature, as also noted by Ragush et al. (2017). The large increase in the sensitivity coefficient of
435 Kl_{O2} at low temperature identifies $CBOD_5$ removal at these low temperatures as being rate limited by the lack of
436 oxygen. The observation of the importance of Kl_{O2} at low temperature highlights the lack of impact of
437 phytoplankton at a temperature of 5 $^{\circ}$C, as well as illustrates the importance of phytoplankton in a system intended
438 to remove $CBOD_5$. The BGS parameter, the bacterial carrying capacity, was more sensitive at an increased
439 temperature of 15 $^{\circ}$C compared to 5 $^{\circ}$C. This would suggest that once the limitation of oxygen has been removed in
440 WSPs, it is the activity (and size) of the bacterial community that will be the limiter of the $CBOD_5$ treatment rate.

441 4 Conclusion

442 Our model successfully linked aspects of ecosystem models (phytoplankton growth, irradiance) with wastewater
443 treatment models (bacterial growth, $CBOD_5$) though the stoichiometry of reactions utilizing carbon dioxide and
444 oxygen to create a model of arctic WSPs. Our efforts to model WSPs in the arctic shed light on the unique aspect of
445 modeling phytoplankton under poorly mixed conditions, and we demonstrated, that in a poorly mixed system,
446 approaching phytoplankton growth functions through a paradigm of growth optimization is a viable path to
447 developing functions that are representative. A local sensitivity analysis was performed and illustrated the

importance of phytoplankton for the removal of $CBOD_5$ and the development of facultative conditions (> 2 mg/l DO).

Our box model of the photic zone of WSPs operating under arctic conditions had the ability to predict the trends in $CBOD_5$ and DO concentrations presented in Ragush et al. (2017) for different light and irradiance conditions. Highlighted in the study, is that the difference in the phytoplankton growth rate was largely responsible for WSP treatment performance in the temperature range of 5 – 15^{o}C. The $CBOD_5$ removal rate was oxygen limited in instances when phytoplankton concentrations were small, and point to the requirement of either supporting the phytoplankton population's growth under these cold conditions or supplementing oxygen in WSPs with aeration to achieve effective $CBOD_5$ treatment. In terms of supporting the phytoplankton population's growth, the most logical method is increasing the temperature in these systems, and the most intuitive way of potentially doing so is providing shallow summer treatment cells (less than 1.5 m deep).

5 Acknowledgements

The authors would like to thank the Government of Nunavut and the Natural Science and Engineering Research Council of Canada for their financial support of this research.

References

Banks, C. J., Koloskov, G. B., Lock, A. C., & Heaven, S. (2003). A computer simlulation of the oxygen balance in a cold climate winter storage WSP during the critical spring warm-up period. *Water Science and Technology, 48*(2), 189-195.

Behrenfeld, M. J., & Falkowski, P. g. (1997). A consumer's guide to phytoplankton primary productivity models. *Limnology and Oceanography, 42*(7), 1479-1491. doi:10.4319/lo.1997.42.7.1479

Benson, B. B., & Krause, D. J. (1984). The concentration and isotopic fractionation of oxygen dissolved in freshwater and seawater in equilibrium with atmosphere. *Limnology and Oceography, 29*(3), 620-632. doi:10.4319/lo.1984.29.3.0620

Beran, B., & Kargi, F. (2005). A dynamic mathmatical model for wastewater stabilization ponds. *Ecological Modelling, 181*(1), 39-57. doi:10.1016/j.ecolmodel.2004.06.022

Boogerd, F., Bos, P., Kuenen, J., Heijnen, J., & van der Lans, R. (1990). Oxygen and carbon dioxide mass transfer and the aerobic, autotrophic cultivation of moderate and extreme thermophiles: a case study relate to microbial desulfurization of coal. *Biotechnology and Bioengineering, 35*(11), 1111-1119.

Boyd, C. E. (1973). The chemical oxygen demand of waters and biological materials from ponds. *Transactions of the American Fisherieis Society, 102*(3), 606-611.

Buhr, H., & Miller, S. (1983). A dynamic model of the high-rate algal-bacterial wastewater treatment pond. *Water Research, 17*(1), 29-37. doi:10.1016/0043-1354(83)90283-X

Chu, C. R., & Jirka, G. H. (2003). Wind and stream flow induced reaeration. *Journal of Environmental Engineering, 129*(12), 1129-1136. doi:10.1061/(ASCE)0733-9372(2003)129:12(1129)

Contois, D. (1959). Kinetics of bacterial growth:relationship between oopulation density and specific growthrate of continuous cultures. *Journal of General Microbiology, 21*, 40-50.

Cramer, M., & Myers, J. (198). Nitrate reduction and assimilation in Chlorella pyrenoidsa. *Joural of Genral Physiology*, 93-102.

Cullen, A., & Frey, H. (1999). *Probabilistic Techniques in Exposure Assessment. A handbook for dealing with Variability and Uncertainty in Models and Inputs.* New York and London: Plenum Press.

Dauta, A., Devau, J., Piquemal, F., & Boumnich, L. (1990). Growth rate of four freshwater algae in relation to light and temperature. *Hydrobiologia, 207*(1), 221-226. doi:10.1007/BF00041459

Dawson, R. N., & Grainge, J. (1969). Design criteria for wastewater lagoons in arctic and sub-arctic regions. *Water Pollution Control Federation, 41*(2), 237-246.

Deacon, E. (1977). Gas transfer to and across an air-water interface. *Tellus*, 363-374.

Downing, D. J., Gardner, R. H., & Hoffman, F. O. (1985). An examination of response-surface methodologies for uncertainty analysis in assessment models. *Technometrics, 27*(2), 151-163. doi:10.2307/1268763

Elmore, H., & West, W. (1961). Effect of water temperature on stream reaeration. *Joural of Sanitization Engineering Divistion - American Society of Civil Engineers*(87), 59-71.

Fogg, G. E. (1953). *The Metabolism of Algae.* New York: John Wiley & Sons.

Fritz, J. J., Middleton, A. C., & Meredith, D. D. (1979). Dynamic process modeling of wastewater stabilization ponds. *Journal of the Water Pollution Control Federation, 51*(11), 2724-2743.

Gaudy Jr., A., Bhalta, M., & Gaudy, E. (1964). Use of chemical oxygen demandvalues of bacterial cells in waste-water purification. *Applied Microbiology, 12*(3), 254-260.

Government of Canada. (2012, June 29). *Justice laws website*. Retrieved from Government of Canada: http://laws-lois.justice.gc.ca/eng/regulations/SOR-2012-139/FullText.html

Heinke, G., Smith, D., & Finch, G. (1991). Guidelines for planning and design of wastewater lagoon systems in cold climates. *Canadian Journal of Civil Engineering, 18*(4), 556-566.

Henze, M. (1979). Sewage Treatment by Activated Sludge - A model with emphasis on oyxgen consumption and sludge composition. *Proceedings of a Post-Conference Seminar held at the Technical University of Denmark* (pp. 41-60). Oxford: Pergamon Press.

Huisman, J., & Weissing, F. J. (1994). Light-limited growth and competion for light in well-mixed aquatic enviroments: An elementary model. *Ecology, 75*(2), 507-520. doi:10.2307/1939554

Klausmeier, C. A., & Litchman, E. (2001). Algal games: the vertical distribution of phytoplankton in poorly mixed water columns. *Limnology and Oceanography, 46*(8), 1998-2007. doi:10.4319/lo.2001.46.8.1998

Klemetson, S. (1983). *Solar Heating of Wastewater Stabilization Ponds.* Fort Collins, Colorado: Colorado State University.

Lawrence, A. W., & McCarty, P. L. (1970). Unified basis for biological treatment design and operation. *Journal of Sanitary Engineering Division, 96*(3), 757-778.

Li, Q. P., Franks, P. J., Landry, M. R., Georicke, R., & Taylor, A. G. (2010). Modeling phytoplankton growth rates and chlorophyll to carbon rations in california coastal and pelagic ecosytems. *Journal of Geophysical Research, 115*(G4), 1-12. doi:10.1029/2009JG001111

Long, S. P., & Humphries, S. (1994). Photoinhibition of photosynthesis innature. *Annual Review of Plant Physiology and Plant Molecular Biology, 45,* 633-662. doi:10.1146/annurev.pp.45.060194.003221

Lorenzen, C. J. (1972). Extinction of light in the ocean by phytoplankton. *ICES Journal of Marine Science, 34*(2), 262-267. doi:10.1093/icesjms/34.2.262

McKinney, R. E. (2004). *Environmental Pollution Control Microbiology.* New York: CRC Press.

Mellard, J. P., Yoshiyama, K., Litchman, E., & Klausmeier, C. A. (2011). The vertical distribution of phytoplankton in stratisfied water columns. *Journal of Theoretical Biology, 269*(1), 16-30. doi:10.1016/j/jtbi.2010.09.041

Metcalf & Eddy. (2003). *Wastewater Engineering treatment and reuse: Fourth Edition.* New York: McGraw-Hill.

Moreno-Grau, S., Garcia-Sanchez, A., Moreno-Clavel, J., Serrano-aniorte, J., & Moreno-Grau, M. (1996). A mathematical model for waste water stabilization ponds with macrophytes and microphytes. *Ecological Modelling, 91*(1-3), 77-103. doi:10.1016/0304-3800(95)00168-9

National Institute of Standards and Techology. (2015, 02 09). *Carbon Dioxide.* Retrieved from NIST Chemistry WebBook: http://webbook.nist.gov/chemistry/

Nunavut Water Board. (2015, July 10). *Public Registry ftp.* Retrieved from Nunavut Water Board: http://www.nwb-oen.ca

Orhon, D., & Artan, N. (1994). *Modelling of Activated Sludge Systems.* Lancaster: Technomic Publishing.

Ragush, C. M., Poltarowicz, J. M., Lywood, J., Gagnon, G. A., Truestrup-Hansen, L., & Jamieson, R. C. (2017). Understanding the Influence of light, temperature and organic loading rates on oxygen dynamics and carbon removal in wastewater stabilization ponds operating in arctic environments. *Ecological Engineering, 98,* 91-97. doi:10.1016/j.ecoleng.2016.10.03

Ragush, C. M., Schmidt, J. J., Kroksek, W. H., Gagnon, G. A., Truelstrup-Hansen, L., & Jamieson, R. C. (2015). Performance of municipal waste stabilization ponds in the Canadian Arctic. *Ecological Engineering, 83,* 413-421. doi:10.1016/j.ecoleng.2015.07.008

Salehi, F., Prasher, S., Amin, S., Madani, A., Jebelli, S., Ramaswamy, H., & Drury, C. (2000). Prediction of annual nitrate-N losses in drain outflows with artificial neural networks. *Transaction of ASAE, 43*(5), 1137-1143.

Schnoor, J. L. (1996). *Environmental Modeling: Fate and Transport of Pollutants in Water, Air and Soil.* New York: John Wiley & Sons.

Shilton, A. (2005). *Pond Treatment Technology.* London: IWA.

US EPA. (1983). *Design Manual: Municipal Wastewater Stabilization Ponds.* Environmental Protection Agency.

Zweitering, M., Jongenburger, I., Rombouts, F., & RIET, K. V. (1990). Modeling of bacterial growth curve. *Applied and Environmental Microbiology*, *56*(6), 1875-1881. doi:0099-2240/90/061875-07$02.00/0